J Chem Technol Biotechnol 79:1293–1300 (online: 2004)
DOI: 10.1002/jctb.1128

Characteristics of photocatalytic oxidation of gaseous 2-propanol using thin-film TiO_2 photocatalyst

Chiu-Ping Chang,[1,2]* Jong-Nan Chen[1] and Ming-Chun Lu[3]

[1]Institute of Environmental Engineering, National Chiao Tung University, Hsinchu 300, Taiwan
[2]Department of Environmental Engineering and Health, Yuanpei University of Science and Technology, 306, Yuanpei St, Hsinchu 300, Taiwan
[3]Department of Environmental Resources Management, Chia Nan University of Pharmacy and Science, Tainan 717, Taiwan

Abstract: This work presents a photocatalysis-based method to treat and purify air because of its broad applicability to common, oxidizable, air contaminants. The effect of oxygen content, temperature, water vapor, and 2-propanol concentration on the TiO_2 surface was investigated. The rate of 2-propanol decomposition increased with increasing the oxygen content, but was reduced at temperatures higher than 100 °C. When water vapor concentration was in the range of 10–355 mmol m^{-3}, the rate of 2-propanol decomposition was proportional to the water content. However, an opposite result was observed at a higher concentration of water vapor. 2-Propanol was photooxidized to acetone, and eventually to carbon dioxide and water. The kinetic model of 2-propanol photooxidation was successfully developed by the competitive Langmuir–Hinshelwood rate form, incorporating the inhibition effect coming from the formation of acetone.

Keywords: photocatalysis; titanium dioxide; kinetics; 2-propanol; acetone

NOTATION

C_a	Acetone concentration (mmol m^{-3})
C_{a0}	Initial concentration of acetone (mmol m^{-3})
C_{CO_2}	Carbon dioxide concentration (mmol m^{-3})
C_p	2-Propanol concentration (mmol m^{-3})
C_{p0}	Initial concentration of 2-propanol (mmol m^{-3})
k_a	Reaction rate constant of acetone (mmol m^{-3} s^{-1})
k_p	Reaction rate constant of 2-propanol (mmol m^{-3} s^{-1})
K_a	Adsorption equilibrium constant of acetone (m^3 mmol^{-1})
K_p	Adsorption equilibrium constant of 2-propanol (m^3 mmol^{-1})
r_a	Reaction rate of acetone (mmol m^{-3} s^{-1})
r_{a0}	Initial reaction rate of acetone (mmol m^{-3} s^{-1})
r_{CO_2}	Reaction rate of CO_2 (mmol m^{-3} s^{-1})
r_p	Reaction rate of 2-propanol (mmol m^{-3} s^{-1})
r_{p0}	Initial reaction rate of 2-propanol (mmol m^{-3} s^{-1})
t	Reaction time (s)
α	Fraction of directly oxidized from adsorbed 2-propanol to carbon dioxide.

1 INTRODUCTION

The interest in heterogeneous photocatalysis to remove trace organic compounds present in air exhaust streams and in indoor environments is intense and increasing. Heterogeneous photocatalysis is a process in which the illumination of an oxide semiconductor, usually the anatase form of titanium dioxide, creates photoexcited electrons (e^-) and holes (h^+). The attractive advantages of this technology are: (i) photocatalytic oxidation can proceed at ambient temperature and pressure; (ii) the excitation source can be sunlight or low-cost fluorescent light sources; (iii) photocatalysts are generally nontoxic, inexpensive, and chemically and physically stable; and (iv) final oxidation products are usually innocuous. The photocatalytic oxidation of single compounds, namely alkanes,[1] alkenes,[2] alcohols,[3–7] ketones,[8–10] aromatics[10–12] and halogenates[13–15] has been previously reported.

Volatile organic compounds (VOCs) can be vaporized at significant rates. Some are toxic and carcinogenic, and are regulated individually as hazardous pollutants.[16] The serious problem related to the emission of VOCs is that they participate

* Correspondence to: Chiu-Ping Chang, Department of Environmental Engineering and Health, Yuanpei University of Science and Technology, 306, Yuanpei St, Hsinchu 300, Taiwan
E-mail: Changcp@mail.yust.edu.tw
Contract/grant sponsor: National Science Council, Taiwan, ROC; contract/grant number: NSC 91-2211-E009-031
(*Received 30 September 2003; revised version received 25 April 2004; accepted 23 June 2004*)
Published online 7 September 2004

in the photochemical reaction and also in the formation of photochemical oxidants, such as ozone and peroxyacetyl nitrate.[17] 2-Propanol, along with other alcohols, is a major contaminant in indoor air and industrial air streams. It is also an important surface probe for titanium dioxide photocatalytic reactions.[4,7,18–22] Larson *et al*[20] indicated that the photocatalytic oxidation of 2-propanol proceeded through acetone as an intermediate, followed by the slow oxidation of acetone to final products, CO_2 and H_2O. Xu and Raftery[7] proposed that the photooxidation of 2-propanol proceeded along two parallel routes. The first route occurred through the formation of acetone, and was followed by the aldol condensation of acetone to form mesityl oxide. The second one occurred through the complete oxidation of 2-propoxide to CO_2. Ohko and colleagues[4,18] studied the kinetics of the 2-propanol oxidation under light-limited and mass transport-limited conditions. Xu *et al*[22] found that the decay rate of acetone during acetone photooxidation was much faster than that of acetone formed as an intermediate during 2-propanol photooxidation. However, these studies are insufficient to evaluate the kinetics of competitive oxidation between 2-propanol and acetone.

In this study, Degussa P25 titanium dioxide was used due to its high activity and commercial availability. Firstly, we found the optimum condition for the removal of 2-propanol as a function of inlet concentration of 2-propanol, water vapor, oxygen content, and reaction temperature. Afterwards, a single-site Langmuir–Hinshelwood kinetic model was developed. It incorporated the competitive oxidation of 2-propanol and intermediates. Kinetic parameters for each component were determined separately, and then combined to produce a kinetic model, attempting to predict the kinetics of 2-propanol degradation and by-product (acetone and carbon dioxide) formation. The kinetic modeling results were compared with experimental data, and then a modified Langmuir–Hinshelwood kinetic model was proposed.

2 EXPERIMENTAL

2.1 Apparatus

The annular reactor made of Pyrex glass is represented in Fig 1a. The width of the annulus varied from 1.5 to 1.85 cm and the length was 30 cm. The total volume of the reactor was 110 cm^3. The photocatalytic system is displayed in Fig 1b. Illumination was provided by a 10 W black light lamp (Sankyo Denki Japan-BLB) with a maximum light intensity output at 365 nm. The light intensity was measured by UV spectrometry (International Light, IL-1700) and was 3.0 mW cm^{-2} on the surface of TiO_2. 2-Propanol and water were drawn by syringes to stainless steel tubes wrapped with heating tape for vaporization. The concentrations of 2-propanol and water were controlled by the syringe pumps (KD Scientific, Model 250). The mass flow controller (MKS, Model 247C) controlled the flow rates of nitrogen and oxygen. The gas flow of nitrogen and oxygen carried gas-phase 2-propanol and water into the reactor. The reactor was wrapped with heating tape to maintain the reaction temperature.

Typical experiments followed the steps: (1) close the valves at the two sides of the reactor when the concentration of 2-propanol stabilized; (2) turn on the UV lamp for 10 s; (3) insert a 10 cm^3 syringe into the sampling port to adequately mix the gas in the reactor; (4) use a gas-tight syringe to sample from the sampling port; (5) repeat steps 2–4 until the experiment is completed.

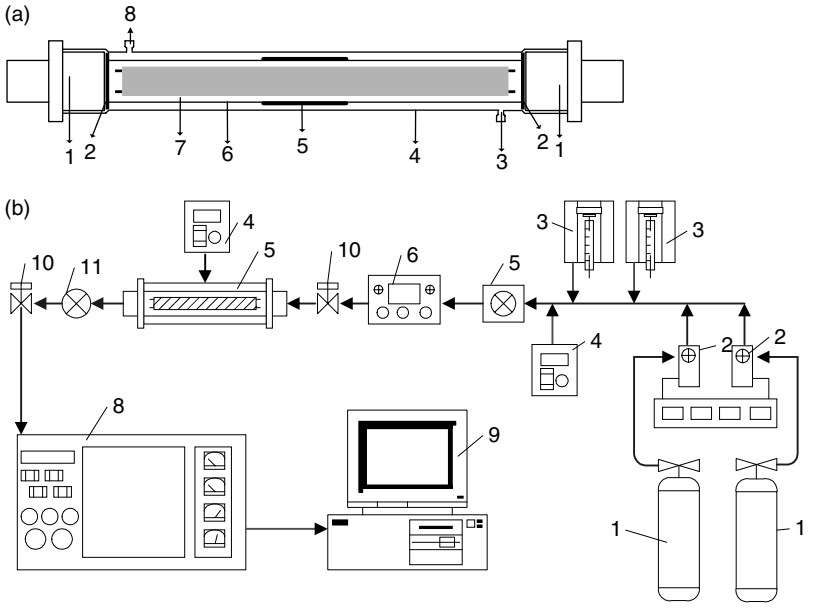

Figure 1. (a) Schematic diagram of reactor. 1, Teflon screw bolt; 2, 'O'-ring; 3, gas inlet; 4, outer tube; 5, TiO_2 film; 6, inner tube; 7, UV light; 8, gas outlet. (b) Set-up of experimental apparatus. 1, Gas cylinder (N_2 and O_2); 2, mass flow controller; 3, syringe pump; 4, heater; 5, mixer; 6, dewpoint sensor; 7, photocatalytic reactor; 8, GC/FID; 9, computer; 10, gas gate; 11, sampling port.

2.2 Photocatalyst

The catalyst used in this study was Degussa P-25 titanium dioxide. The surface area of the powder is $50 \pm 15\,m^2\,g^{-1}$ (BET). The TiO_2 thin-film catalyst was prepared using a spread-coating method. It was coated on the outer surface of the inner tube using a well-mixed slurry of 10 wt% TiO_2 in deionized water. The area of catalyst film was $52\,cm^2$ (the length of spread = 5.5 cm). The TiO_2-coated tube was then heated at 110 °C for 1.5 h. A TiO_2 loading density of $0.09\,mg\,cm^{-2}$ was obtained by weighing the tube before and after the coating. Scanning electron microscopy (SEM, Hitachi S-4300) images are shown in Fig 2, which shows top (a) and cross-sectional (b) views. The film consists of small crystalline particles with an average diameter of about 40 nm. The thickness of the TiO_2 film was approximately 0.6 μm. The surface roughness of the film was examined by a topography measurement instrument (Taylor Hobson, Talyscan 150). The average roughness of the TiO_2 film was 0.22 μm.

2.3 Analytical methods

The 2-propanol and acetone concentrations were analyzed by a China GC-9800F gas chromatograph equipped with a flame ionization detector (FID) and a Cobalwax packed column (2.0 m long × 3.2 mm od). Hydrogen was used as the carrier gas.

Carbon dioxide formed as a result of 2-propanol photooxidation was analyzed with an FID and a Porapak Q column (2.0 m long × 3.2 mm od) after converting CO_2 to CH_4 through a Ni-catalyst methanizer. The temperatures of the Porapak Q column and methanizer were 60 °C and 370 °C, respectively.

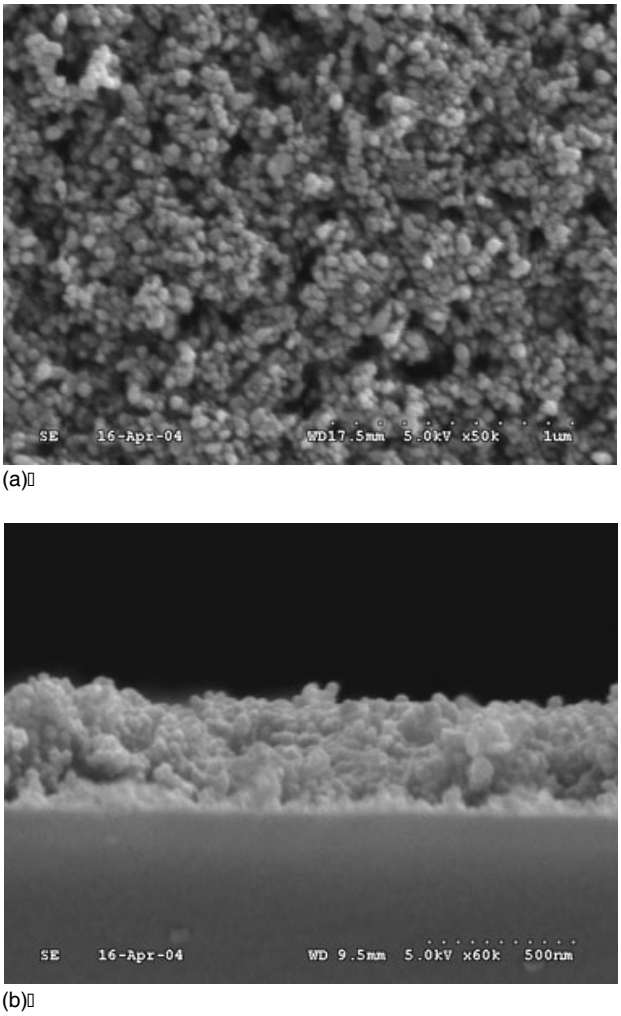

Figure 2. SEM photographs of (a) top and (b) cross-sectional views of the TiO_2 film on the Pyrex glass tube.

3 RESULTS AND DISCUSSION

3.1 Effect of initial concentration

The variation of 2-propanol concentration in air with the reaction time for five different initial concentration levels is shown in Fig 3; in these experiments the temperature was 100 °C, the oxygen content was 20%, and the water vapor content was $10.3\,mmol\,m^{-3}$. The intensity of the UV irradiation on the catalyst surface was $3.0\,mW\,cm^{-2}$. Because the reaction area was large ($52\,cm^2$) and the total volume of reactant was small ($110\,cm^3$), 2-propanol can be destroyed quickly under these conditions.

In general, the kinetics of the photocatalytic degradation of organics would follow the Langmuir–Hinshelwood model (eqn (1)).[10]

$$r_p = \frac{k_p K_p C_p}{1 + K_p C_p} \tag{1}$$

Owing to the complex mechanism of photocatalytic oxidation, kinetic modeling of the reaction is usually limited to the analysis of the initial rate of degradation. This can be obtained from the initial slope and the initial concentration of 2-propanol in an experiment in which the variation of the 2-propanol concentration is measured as a function of time. As can be seen in Fig 3, the initial slope increased with increasing the initial concentration, but remained almost constant beyond

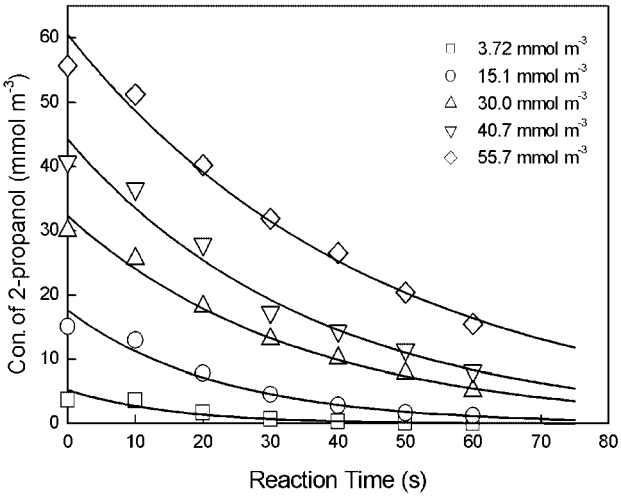

Figure 3. Effect of 2-propanol concentration on photocatalytic degradation (experimental conditions: t = 100 °C; oxygen = 20%; water vapor = $10.3\,mmol\,m^{-3}$).

a certain concentration. Rearranging eqn (1) for initial rate analysis gives:

$$\frac{1}{r_{p0}} = \frac{1}{k_p} + \frac{1}{k_p K_p} / \frac{1}{C_{p0}} \quad (2)$$

A plot of the reciprocal initial rate ($1/r_0$) versus the reciprocal initial concentration ($1/C_0$) can be represented by a straight line (Fig 4), with a linear least-squares fit (solid line, Fig 4) having a slope of 13.1 and an intercept of 0.613 ($r^2 = 0.99$). From eqn (2) the slope and intercept are given by:

$$\text{intercept} = \frac{1}{k_p} \quad (3)$$

$$\text{slope} = \frac{1}{k_p K_p} \quad (4)$$

The kinetic parameters k_p and K_p are 1.63 mmol m^{-3} - s^{-1} and 0.0469 m^3 $mmol^{-1}$, respectively. Figure 5 describes the initial rate as a function of initial concentration of 2-propanol. By substituting the k_p and K_p values into eqn (1), the analytical relationship between r_{p0} and C_{p0} is obtained. The solid line drawn in Fig 5 represents this relationship; a good fitting of the model to the experimental data may be observed. It is indicated that the photocatalytic oxidation of 2-propanol was through the physical adsorption of 2-propanol on the active sties of the titanium dioxide. The higher the concentration of gas-phase 2-propanol, the more adsorbed molecules on the catalyst surface, unless the saturation point is approached. Therefore, with increasing initial concentration of 2-propanol, the reaction rate of 2-propanol increased.

3.2 Effect of temperature

Temperature is one of the important factors in gas–solid heterogeneous photocatalytic reactions. Photocatalytic degradation of trichloroethylene and

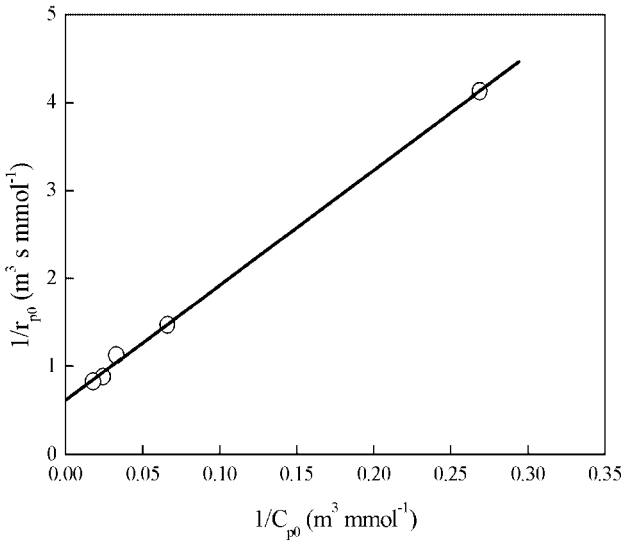

Figure 4. Linearized reciprocal kinetic plot for the photocatalytic degradation of 2-propanol.

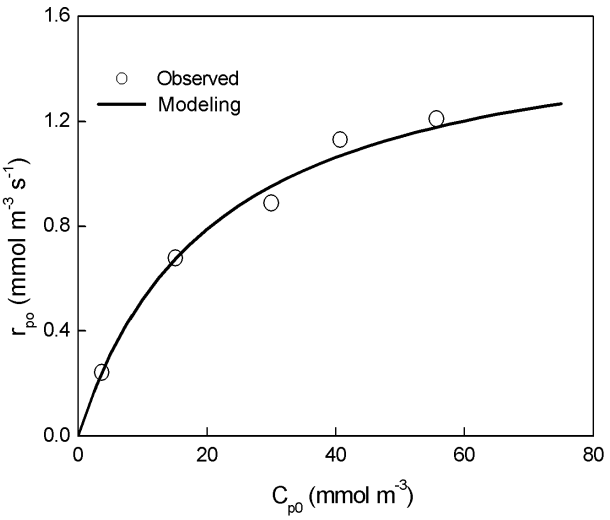

Figure 5. The initial reaction rate for the photodegradation of 2-propanol at different initial concentrations (experimental conditions: $T = 100\,°C$; oxygen = 20%; water vapor = 10.3 mmol m^{-3}).

methanol was more effective at a moderate temperature than at higher temperatures.[23] The yield of acetone from 2-propanol oxidation was maximized at a surface temperature of 77 °C and decreased to low values at −23 °C and 327 °C.[24] To explore the effect of temperature, variable temperatures in the range from 25 °C to 200 °C were investigated at a fixed concentration of 2-propanol. Figure 6 shows that the initial reaction rate of 2-propanol oxidation increased with increasing temperatures ranging from 25 °C to 100 °C. Above 100 °C, the initial reaction rate was reduced with increasing temperature. At low temperature, the desorption of product can be the rate-limiting step,[25] and acetone was the major intermediate of 2-propanol photooxidation. The yield of acetone from 2-propanol oxidation was limited by the desorption of acetone at low temperature.[24] Raising the temperature accelerated the desorption of acetone. Hence, increasing temperature increased the reaction rate of 2-propanol when reaction temperatures were below 100 °C. In contrast, adsorption of reactant would be the rate-determining step at high temperature.[23] The surface coverage of the reactant decreases with increasing temperature.[19,25] Therefore, the photocatalytic rate of 2-propanol was reduced when reaction temperatures were above 100 °C.

3.3 Effect of oxygen content

Activation of TiO_2 can be achieved through the adsorption of a photon of ultraviolet light ($\lambda <$ 365 nm), which results in the promotion of an electron, e^-, from the valence band to conduction band, with the simultaneous generation of a hole, h^+, in the valence band (eqn (5)).

$$TiO_2 \xrightarrow{h\nu(\lambda < 365\ nm)} h_{vb}^{+} + e_{cb}^{-} \quad (5)$$

The holes may be depleted directly by the organics or trapped by hydroxyl ions forming hydroxyl radicals

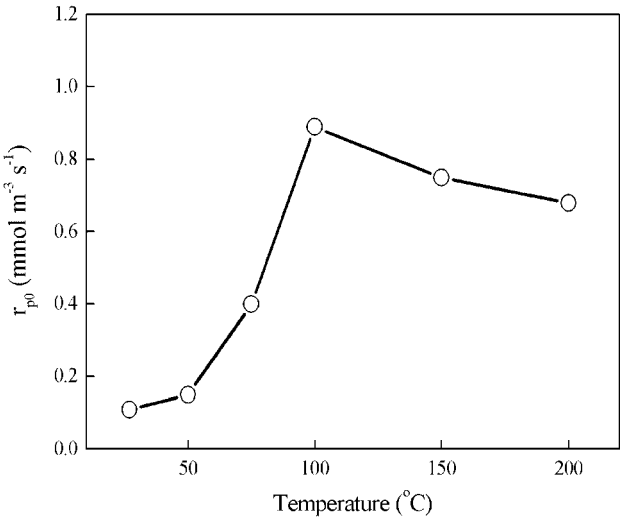

Figure 6. The variation of initial reaction rate constants under different temperatures (experimental conditions: water vapor = 10.3 mmol m^{-3}; oxygen = 20%; C_{p0} = 30.3mmol m^{-3}).

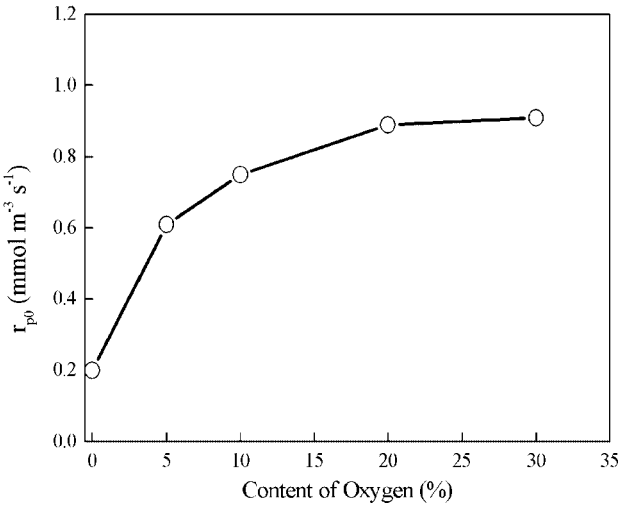

Figure 7. The variation of initial reaction rate under different oxygen contents (experimental conditions: T = 100 °C; water vapor = 10.3 mmol m^{-3}; C_{p0} = 30.3 mmol m^{-3}).

(eqn (6)).

$$h^+_{vb} + H_2O_{ads} \longrightarrow OH\bullet_{ads} + H^+ \qquad (6)$$

The holes lose the capacity of oxidation if they recombine with the electrons. Oxygen is an electron acceptor. The electron may be trapped by oxygen to reduce the probability for recombination of electron/hole pairs (eqn (7)).

$$O_{2(ads)} + e^- \longrightarrow O^-_{2(ads)} \qquad (7)$$

Oxygen was important for the complete oxidation of 2-propanol in the UV/TiO_2 system. When the oxygen concentration increased from 0.003% to 3%, the extent of 2-propanol mineralization was promoted from 3.3% to 42%.[20] For acetone, the degradation ratio increased from 20% to 70% while increasing the oxygen content from 0% to 5% (v/v).[26] Figure 7 reveals that the initial reaction rate increased as the oxygen content increased from 0% to 20% when the temperature was 100 °C, water vapor content was 10.3 mmol m^{-3}, and 2-propanol content was 30.3 mmol m^{-3}. The initial reaction rate reached a stable level when the oxygen content was higher than 20%. When the oxygen concentration was reduced to 0%, the photocatalytic oxidation of 2-propanol could still take place, due to the participation of the holes or hydroxyl radicals (eqns (5) and (6)). The probability for the recombination of electron/hole pairs could be reduced because gas-phase oxygen adsorbed on the surface reacts with electrons to form super-oxide ions (O_2^-; eqn (7)). Additionally, super-oxide ions are highly reactive species that can oxidize 2-propanol. The amount of adsorbed oxygen on the TiO_2 surface increases with increased concentration of gaseous oxygen. Consequently, increased oxygen content can promote the photocatalytic oxidation of 2-propanol. However, the surface site was saturated with adsorbed oxygen when the oxygen content was high, leading to the result that increased gaseous oxygen did not increase the amount of adsorbed oxygen. Fortunately, the adsorption sites on oxygen and organics were different, oxygen does not inhibit the oxidation of 2-propanol at high oxygen content.[27]

3.4 Effect of water vapor

Actually, the treatment of gaseous 2-propanol is likely to be performed in the presence of water vapor. The influence of water vapor on the photooxidation is complex since water plays an important role in the formation of the active species (OH•, eqn (6)). However, the adsorbed water is an effective electron–hole recombination center, leading to less efficient photoactivity.[28] To examine the effect of water vapor, different quantities of water vapor were applied to a fixed concentration of 2-propanol. Figure 8 shows the initial reaction rate versus initial water vapor concentration, varying from 10 to 1800 mmol m^{-3}. The photocatalytic degradation rate was enhanced by water vapor with concentrations up to 355 mmol m^{-3}, and inhibited above 355 mmol m^{-3}. In this case, the reaction of 2-propanol and surface hydroxyl radicals during the oxidation process caused the depletion of these hydroxyl radicals. The oxidation rate of 2-propanol was raised because the production of hydroxyl radical increased with increasing water vapor. Additionally, the adsorption sites for water and 2-propanol were the same.[27] Hence, water vapor competed with 2-propanol for adsorption sites on the catalyst's surface. The concentration of water vapor was much higher than that of 2-propanol at high water vapor. This is beneficial to the adsorption of water, leading to the reduction of 2-propanol oxidation at high concentration of water vapor.

3.5 Competitive oxidation of 2-propanol and acetone

The mechanism for 2-propanol photooxidation on TiO_2/PVG (porous Vycor glass) is reported to be

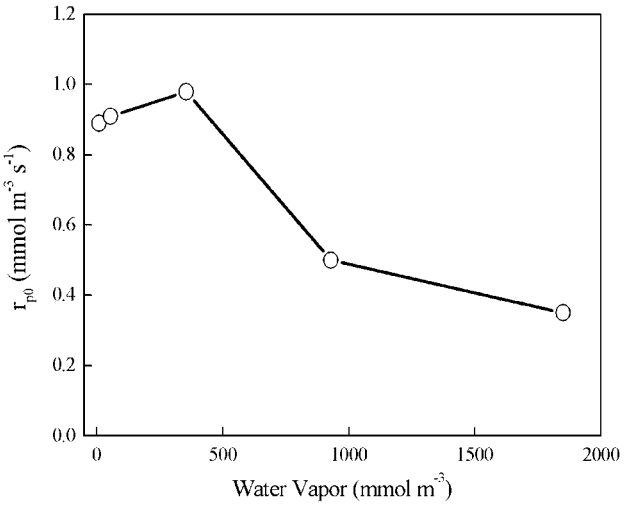

Figure 8. The variation of initial reaction rate under different humidities (experimental conditions: $T = 100\,^{\circ}C$; oxygen = 20%; $C_{p0} = 30.3\,mmol\,m^{-3}$).

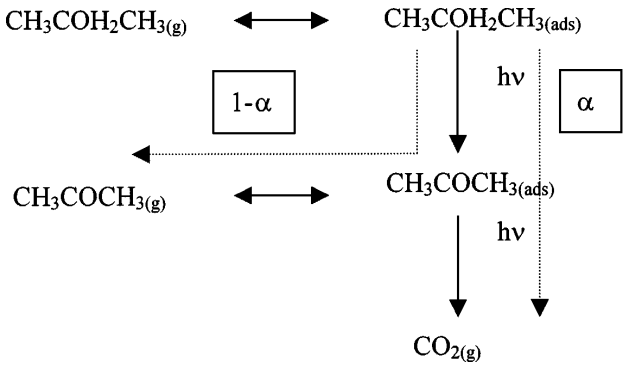

Figure 9. Photocatalytic degradation pathway of 2-propanol.

2-propanol$_{(ads)}$ → acetone$_{(ads)}$→→carbon dioxide.[7] In this study, acetone and carbon dioxide were detected in the photocatalytic oxidation of 2-propanol. Hence, the pathway of 2-propanol degradation through an observed gaseous intermediate, acetone, to the final product, carbon dioxide was proposed (see Fig 9). The photocatalytic destruction of 2-propanol on the TiO_2 is assumed to follow a single-site Langmuir–Hinshelwood rate form, where the 2-propanol reactant and partially oxidized intermediate compete for surface sites, and therefore inhibit the photooxidation rates of each other. The simplifying assumption is that the product (carbon dioxide) does not inhibit the photocatalytic rates. The resulting rate equation for 2-propanol is:

$$r_p = \frac{k_p K_p C_p}{1 + K_p C_p + K_a C_a} \tag{8}$$

The rate of change in number of moles of the reactant due to reaction is dN_p/dt. Based on unit volume of reactor, the rate of reaction is defined as follows:

$$r_p = -\frac{1}{V}\frac{dN_p}{dt} = -\frac{dC_p}{dt} \tag{9}$$

Thus, the rate equation becomes:

$$\frac{dC_p}{dt} = -\frac{k_p K_p C_p}{1 + K_p C_p + K_a C_a} \tag{10}$$

For acetone, the net rate for acetone formation during 2-propanol oxidation is:

$$r_a = \frac{dC_a}{dt} = \frac{k_p K_p C_p - k_a K_a C_a}{1 + K_p C_p + K_a C_a} \tag{11}$$

If one mole of acetone is completely oxidized, three moles of CO_2 are produced. Thus, the rate equation for CO_2 formation is:

$$r_{CO_2} = \frac{dC_{co_2}}{dt} = \frac{3k_a K_a C_a}{1 + K_p C_p + K_a C_a} \tag{12}$$

The 2-propanol kinetic parameters, k_p and K_p, are now given from initial-rate data of 2-propanol described above. A plot of the initial reaction rate of acetone oxidation versus the initial acetone concentration, similar to 2-propanol, can be represented by a straight line (Fig 10), with a linear least-squares fit (solid line) having a slope of 22.18 and an intercept of 3.10. The values of k_a and K_a are $0.322\,mmol\,m^{-3}\,s^{-1}$ and $0.140\,m^3\,mmol^{-1}$, respectively. Equations (10)–(12) should now construct a predictive model for 2-propanol oxidation over a time course where two contaminants, 2-propanol and acetone, are present. To verify this hypothesis, the model was evaluated at the same conditions as that of the 2-propanol experiments; the model predictions and the experiments are compared in Fig 11. The predictive model described well the variation of 2-propanol. However, acetone and carbon dioxide did not vary as expected. A simple modification to the reaction scheme of Fig 9 improves the fit of the model: a fraction 'α' of the adsorbed 2-propanol is allowed to be oxidized to carbon dioxide via a mechanism that does not involve an adsorbed acetone intermediate. Hence eqns (11) and (12) were revised to eqns (13) and (14), respectively.

$$\frac{dC_a}{dt} = \frac{(1-\alpha)k_p K_p C_p - k_a K_a C_a}{1 + K_p C_p + K_a C_a} \tag{13}$$

$$\frac{dC_{CO_2}}{dt} = \frac{3(\alpha k_p K_p C_p + k_a K_a C_a)}{1 + K_p C_p + K_a C_a} \tag{14}$$

The fraction (α) was determined using trial and error analysis and gave $\alpha = 0.25$. Figure 12 compares the revised model predictions and the experiments. The revised model predicts the variation of 2-propanol oxidation as well as the acetone formation with reaction time. The amounts of carbon dioxide production analyzed by experiment were lower than that by the model predicted before 60 s. In this case, the adsorbed acetone formed surface-adsorbed species, for example, diacetone alcohol, mesityl oxide, propylene oxide, and acetic acid; they were subsequently oxidized photocatalytically to carbon

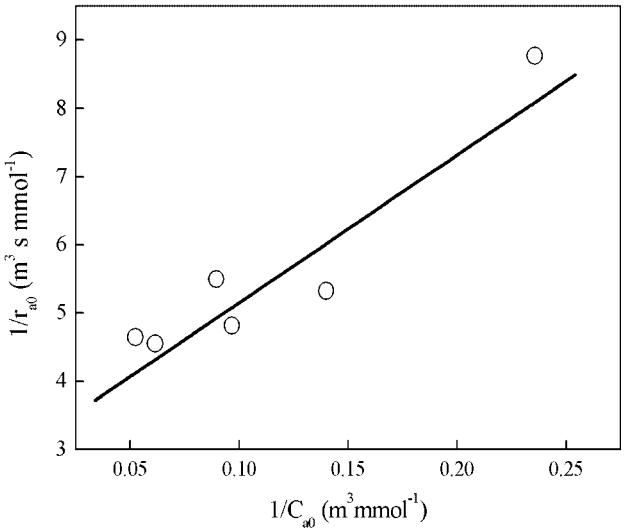

Figure 10. Linearized reciprocal kinetic plot for the photocatalytic degradation of acetone.

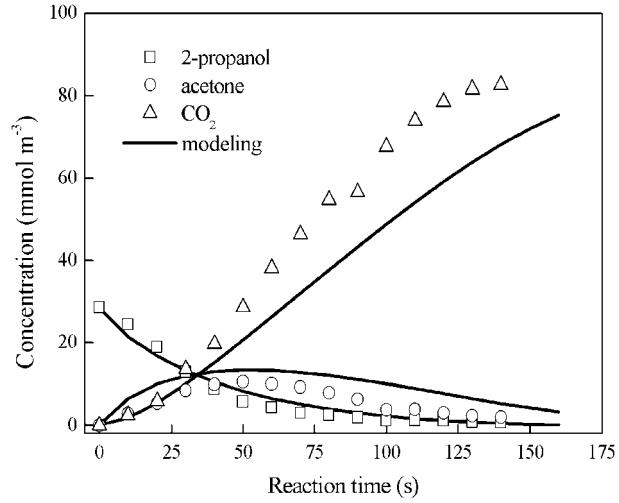

Figure 11. 2-Propanol photooxidation, experimental data and predictive model, including intermediate and product evolution (experimental conditions: $T = 100\,°C$; water vapor $= 10.3\,mmol\,m^{-3}$; oxygen $= 20\%$; $C_{p0} = 30.3\,mmol\,m^{-3}$).

dioxide.[7] Therefore, the rate of carbon dioxide production was at first slower than predicted.

4 CONCLUSIONS

The photocatalytic degradation of 2-propanol as a function of initial concentration, water vapor, oxygen content, and reaction temperature was investigated using a batch photoreactor. The higher the initial 2-propanol concentration, the faster the reaction rate. The optimum temperature for the 2-propanol oxidation in this study is 100 °C. When the oxygen content was higher than 20%, the reaction rate was almost constant. The photocatalytic oxidation of 2-propanol can take place without the presence of gaseous molecular oxygen. The water vapor enhanced the degradation of 2-propanol at low humidity but inhibited the reaction at high water content. 2-Propanol and the

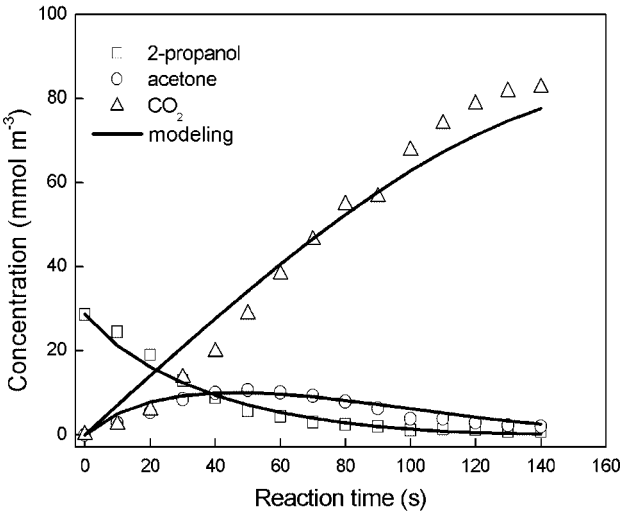

Figure 12. 2-Propanol photooxidation, experimental data and revised predictive model, including intermediate and product evolution.

partially oxidized intermediate, acetone, competed for surface sites, resulting in inhibition of the photooxidation rate of both chemicals. The competitive Langmuir–Hinshelwood type behavior was used to describe the photodegradation reaction.

ACKNOWLEDGMENT

This work has been supported by National Science Council, Taiwan, ROC (Grant NSC 91-2211-E009-031).

REFERENCES

1 Shang J, Du Y and Xu Z, Photocatalytic oxidation of heptane in the gas-phase over TiO_2. *Chemosphere* **46**:93–99 (2002).
2 Obee TN and Hay SO, Effects of moisture and temperature on the photooxidation of ethylene on titania. *Environ Sci Technol* **31**:2034–2038 (1997).
3 Sauer ML and Ollis DF, Photocatalyzed oxidation of ethanol and acetaldehyde in humidified air. *J Catal* **158**:570–582 (1996).
4 Ohko Y and Fujishima A, Kinetic analysis of the photocatalytic degradation of gas-phase 2-propanol under mass transport-limited conditions with a TiO_2 film photocatalyst. *J Phys Chem B* **102**:1724–1729 (1998).
5 Sun R-D, Nakajima A, Watanabe I, Watanabe T and Hashimoto K, TiO_2-coated optical fiber bundles used as a photocatalytic filter for decomposition of gaseous organic compounds. *J Photochem Photobiol A* **136**:111–116 (2000).
6 Benoit-Marquie F, Wilkenhoner U, Simon V and Braun AM, VOC photodegradation at the gas–solid interface of a TiO_2 photocatalyst. part I: 1-butanol and 1-butylamine. *J Photochem Photobiol A* **132**:225–232 (2000).
7 Xu W and Raftery D, Photocatalytic oxidation of 2-propanol on TiO_2 powder and TiO_2 monolayer catalysts studied by solid-state NMR. *J Phys Chem B* **105**:4343–4349 (2001).
8 Xu W and Raftery D, In situ solid-state nuclear magnetic resonance studies of acetone photocatalytic oxidation on titanium oxide surfaces. *J Catal* **204**:110–117 (2001).
9 Choi W, Ko JY, Park H and Chung JS, Investigation on TiO_2-coated optical fibers for gas-phase photocatalytic oxidation of acetone. *Appl Catal B* **31**:209–220 (2001).
10 Peral J and Ollis DF, Heterogeneous photocatalytic oxidation of gas-phase organics for air purification: acetone, 1-butanol,

butyraldehyde, formaldehyde, and *m*-xylene oxidation. *J Catal* **136**:554–565 (1992).
11 Blount MC and Falconer JL, Characterization of adsorbed species on TiO_2 after photocatalytic oxidation of toluene. *J Catal* **200**:21–33 (2001).
12 Einaga H, Futamura S and Ibusuki T, Complete oxidation of benzene in gas phase by platinized titania photocatalysts. *Environ Sci Technol* **35**:1880–1884 (2001).
13 Wang KH, Hsieh YH, Lin CH and Chang CY, The study of the photocatalytic degradation kinetics for dichloroethylene in vapor phase. *Chemosphere* **39**:1371–1384 (1999).
14 S'anchez B, Cardona A, Romero M, Avila P and Bahamonde A, Influence of temperature on gas-phase photo-assisted mineralization of TCE using tubular and monolithic catalysts. *Catal Today* **54**:369–377 (1999).
15 Shen YS and Ku Y, Decomposition of gas-phase trichloroethene by the UV/TiO_2 process in the presence of ozone. *Chemosphere* **46**:101–107 (2002).
16 Nevers ND, Control of volatile organic compounds (VOCs), in *Air Pollution Control Engineering*, ed by Nevers ND. *McGraw-Hill Chemical Engineering Series*, McGraw-Hill Book Co, Singapore, pp 329–330 (2000).
17 Japar SM, Wallington TJ, Rudy SJ and Chang TY, Ozone-forming potential of a series of oxygenated organic compounds. *Environ Sci Technol* **25**:415–420 (1991).
18 Ohko Y, Hashimoto K and Fujishima A, Kinetics of photocatalytic reactions under extremely low-intensity UV illumination on titanium dioxide thin films. *J Phys Chem A* **101**:8057–8062 (1997).
19 Brinkley D and Engel T, Evidence for structure sensitivity in the thermally activated and photocatalytic dehydrogenation of 2-propanol on TiO_2. *J Phys Chem B* **104**:9836–9841 (2000).
20 Larson SA, Widegren JA and Falconer JL, Transient studies of 2-propanol photocatalytic oxidation on titania. *J Catal* **157**:611–625 (1995).
21 Rekoske JE and Barteau MA, Kinetics and selectivity of 2-propanol conversion on oxidized anatase TiO_2. *J Catal* **165**:57–72 (1997).
22 Xu W, Raftery D and Francisco JS, Effect of irradiation sources and oxygen concentration on the photocatalytic oxidation of 2-propanol and acetone studied in situ FTIR. *J Phys Chem B* **107**:4537–4544 (2003).
23 Kim SB, Hwang HT and Hong SC, Photocatalytic degradation of volatile organic compounds at the gas–solid interface of a TiO_2 photocatalyst. *Chemosphere* **48**:437–444 (2002).
24 Brinkley D and Engel T, Photocatalytic dehydrogenation of 2-propanol on TiO_2 (110). *J Phys Chem B* **102**:7596–7605 (1998).
25 Pichat P and Herrmann J-M, Adsorption–desorption, related mobility and reactivity in photocatalysis, in *Photocatalysis: Fundamentals and Applications*, ed by Serpoe N and Pelizzetti E. John Wiley & Sons, Inc, New York, pp 217–250 (1989).
26 Chang C-P, Chen J-N and Lu M-C, Heterogeneous photocatalytic oxidation of acetone for air purification by near UV-irradiated titanium dioxide. *Environ Sci Health A* **38**:1131–1143 (2003).
27 Yamazaki S, Tanaka S and Tsukamoto HS, Kinetic studies of oxidation of ethylene over a TiO_2 photocatalyst. *J Photochem Photobiol A* **121**:55–61 (1999).
28 Linsebigler AL, Lu G and Yates JT, Photocatalysis on TiO_2 surfaces: principles, mechanisms, and selected results. *Chem Rev* **95**:735–758 (1995).